Synchronization of hyperexcitable systems with phase-repulsive coupling

Gábor Balázsi,[1] Ann Cornell-Bell,[2] Alexander B. Neiman,[1] and Frank Moss[1]
[1]*Center for Neurodynamics, University of Missouri–St. Louis, 8001 Natural Bridge Road, St. Louis, Missouri 63121-4499*
[2]*Cognetix, Inc./Viatech Imaging, 158 Main Street, Ivoryton, Connecticut 06442*
(Received 3 May 2001; published 24 September 2001)

We study two-dimensional arrays of FitzHugh-Nagumo elements with nearest-neighbor coupling from the viewpoint of synchronization. The elements are diffusively coupled. By varying the diffusion coefficient from positive to negative values, interesting synchronization patterns are observed. The results of the simulations resemble the intracellular oscillation patterns observed in cultured human epileptic astrocytes. Three measures are proposed to determine the degree of synchronization (or coupling) in both the simulated and the experimental system.

DOI: 10.1103/PhysRevE.64.041912 PACS number(s): 87.10.+e, 87.18.−h

I. INTRODUCTION

Methods of synchronization have become an important tool in nonlinear dynamics. Synchronization is observed in a wide variety of natural and artificial systems, such as pendulum clocks [1], respiration [2–6], circadian rhythms [7,8], lasers [9], flashing of fireflies [10,11], neuronal systems [12–15], etc. Within the vast number of systems exhibiting synchronization, the synchronization of extended systems has recently generated an upsurge of interest. Typical examples include laser arrays [16], oscillating chemical media [17], and clapping in concert halls [18]. Important theoretical investigations have pointed to the phenomena of global synchronization and noise-enhanced propagation in excitable media with phase-attractive coupling [19–22]. Phase-attractive coupling is defined as the tendency of any oscillator in a system to have a phase close to its nearest neighbors'.

There has been a long-time concern for synchronization in excitable systems with phase-repulsive (or delayed) coupling [23–25]. In these systems the oscillators tend to have a phase opposite to their nearest neighbors'. This property is similar, but not equivalent to inhibitory coupling [26,27]. In the case of inhibitory coupling, the ''spike'' generated by any oscillator inhibits the spike generation in its nearest neighbors and has no effect on its neighbors during the recovery period. In the case of phase-repulsive coupling, however, even if the value of the oscillator is near its minimum, this forces the value of its nearest neighbors towards the maximum.

Astrocyte cultures are typical examples of excitable systems. Recent studies refer to calcium wave propagation and synchronization [19,28,29]. Calcium waves are initiated by various factors, such as chemical, mechanical, electrical, etc. stimulation. Calcium waves spread from cell to cell by raising the intracellular calcium concentration of the cells through which the wave passes. Each cell participating in a calcium wave affects its nearest neighbors through tiny connecting channels, called ''gap junctions.'' The cells can also affect their neighbors and communicate calcium waves by releasing into the extracellular space active substances such as neurotransmitters or adenosine triphosphate [30,31].

Intracellular calcium oscillations represent another example from the complicated set of responses generated by astrocytes. They are different from calcium waves in that they have smaller amplitude and are strictly intracellular phenomena (i.e., never spread to neighboring cells). Previous studies claimed no interaction between intracellular calcium oscillations of nearby astrocytes [32]. Here we study pathological (epileptic) astrocyte cultures with the method of stochastic synchronization and show the existence of a nontrivial relationship between the phases of nearby oscillating cells.

The goal of the present study is to analyze the effect of the phase-repulsive coupling on two-dimensional, diffusively coupled FitzHugh-Nagumo arrays. We show that two-dimensional arrays of FitzHugh-Nagumo oscillators with phase-repulsive coupling show properties similar to epileptic astrocyte cultures. First, the properties of FitzHugh-Nagumo equations are briefly presented. Secondly, two-dimensional arrays of FitzHugh-Nagumo oscillators with diffusive coupling are studied, for both positive and negative values of the diffusion coefficient. Finally, the similarities to the experimental system (cultured network of human epileptic astrocytes) are analyzed, and further implications of this study are discussed.

II. METHODS

A. FitzHugh-Nagumo equations

The FitzHugh-Nagumo (FN) equations were originally developed as a simplified model of the Hodgkin-Huxley model for neuron dynamics [33,34]:

$$\epsilon \frac{dv}{dt} = v(a-v)(v-1) - w + c, \tag{1}$$

$$\frac{dw}{dt} = v - dw - b, \tag{2}$$

where the variables are v and w, while the excitability parameter is c. v corresponds to the voltage across the membrane, and w controls the recovery period. In this study, the rest of the parameters were kept constant: $\epsilon = 0.005$, $a = 0.5$, $b = 0.2$, and $d = 1.0$.

Depending on the value of the excitability parameter c the system has two kinds of solutions. If $c > 0.055$ and $c < 0.55$,

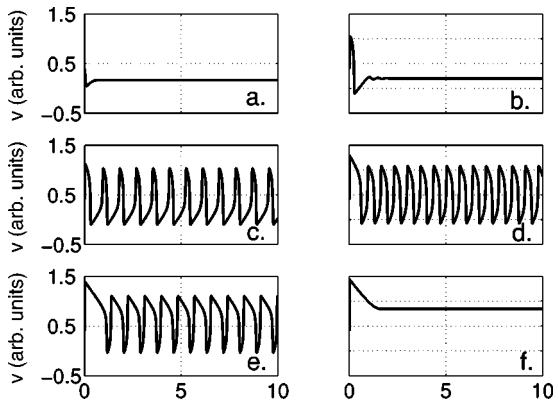

FIG. 1. Solutions of the FN equations (only the first variable is shown) for various values of the excitability parameter c: (a) $c=0.01$, solution relaxes to a stationary value; (b) $c=0.05$, damped oscillations; (c) $c=0.10$, sustained oscillations; (d) $c=0.30$, highest oscillation frequency; (e) $c=0.50$, oscillation frequency decreases; (f) c=0.60, the solution relaxes to a stationary value.

the solution is a limit cycle (independent on the initial value of v and w). On the other hand, if $c<0.055$ or $c>0.55$, the solution relaxes and reaches a stationary value (the time step is $\Delta t=0.005$). In the following simulations the excitability parameter will always be $0.055<c<0.55$, therefore the solution will be oscillatory. The solutions of the equations for different values of the parameter c can be seen on Fig. 1, and the dependence of the oscillation frequency upon the excitability parameter c is shown on Fig. 2.

B. Two-dimensional, diffusively-coupled array

A two-dimensional array of 20×20 FitzHugh-Nagumo elements was considered with free-boundary conditions. If a diffusive term is added to the first equation, each element of this network will influence its nearest neighbors. The discretized form of the system of coupled differential equations becomes

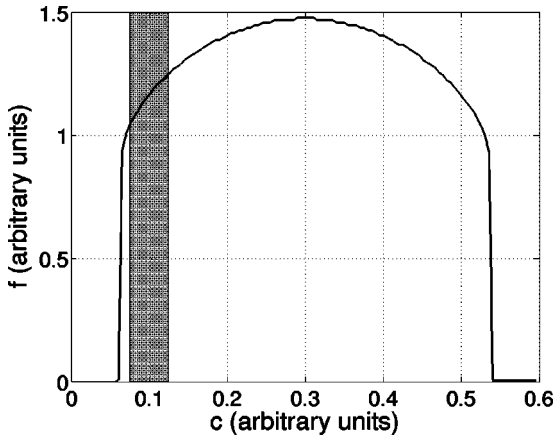

FIG. 2. Natural frequency of the FN oscillator as a function of the excitability parameter c. Notice that the oscillatory regime is $0.055<c<0.55$ and the allowed frequencies have both an upper and a lower limit: they range approximately from 0.95 Hz to 1.5 Hz. The shaded area corresponds to the parameter range of the FitzHugh-Nagumo array discussed in Sec. II B.

$$\epsilon\frac{\Delta v(i,j,t)}{\Delta t}=v(i,j,t)[a-v(i,j,t)][v(i,j,t)-1]-w(i,j,t)+c+N_a\xi(i,j)+D[v(i-1,j,t)+v(i+1,j,t)+v(i,j-1,t)+v(i,j+1,t)-4v(i,j,t)], \quad (3)$$

$$\frac{\Delta w(i,j,t)}{\Delta t}=v(i,j,t)-dw(i,j,t)-b, \quad (4)$$

where $\xi(i,j)$ is a uniformly distributed white noise term. $N_a=0.01$ defines the range of the excitability parameter's domain of variation. As a result, all elements will be in the oscillatory regime and have frequencies close to each other ($c=0.1, N_a=0.01$). D is the diffusion coefficient at every position (i,j) in the lattice; the spatial separation of the oscillators is considered to be $\Delta x=1$.

A similar system has been studied before in Ref. [16], and generation of spiral waves, target waves or global oscillations has been observed. Here we extend this study to the oscillating regime of the FitzHugh-Nagumo system and to negative diffusion coefficients. The studied quantities will be the average synchronization index, the standard deviation of the frequencies and the standard deviation of the sum of time series $v(i,j,t)$.

For a zero diffusion coefficient every element oscillates independently of all the others. For a positive diffusion coefficient, every element tends to minimize the phase difference between itself and its four nearest neighbors. If the diffusion coefficient is negative, every element tends to maximize the phase difference between itself and its four nearest neighbors.

C. Statistical measures

Depending on the initial phases assigned to the oscillators and on the spatial distribution of oscillators with different frequencies, the system showed random spatial fluctuations, spiral wave patterns, and global oscillations for both the phase-attractive and the phase-repulsive coupling. The system was studied for three different sets of initial conditions: Initial conditions *A.* every oscillator started from its maximum; Initial conditions *B.* the initial values of $v(i,j,0)$ were arranged in a chessboard pattern, every second oscillator started from its maximum, every other oscillator started from its minimum; Initial conditions *C*, random initial phases were assigned to every oscillator.

The v values for the three different initial conditions can be seen on Fig. 3. In order to study the synchronization between oscillators in the array, the phase was defined for each of these time series based on marker events, that were chosen to be the upward crossings of the threshold level 0.5 by $v(i,j,t)$. The phase was incremented by 2π for each event and in between the events the phase was approximated by linear interpolation:

$$\phi(t)=2\pi\frac{t-t_k}{t_{k+1}-t_k}+2\pi k, \quad t_k\leqslant t<t_{k+1}, \quad (5)$$

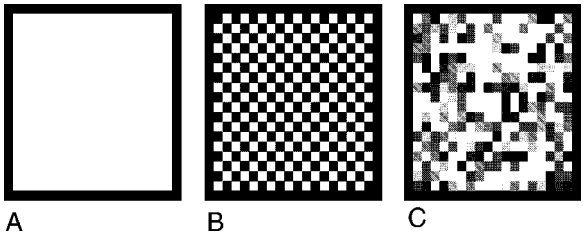

FIG. 3. Initial conditions: *A*, all oscillators start from their peak; *B*, oscillators form a chessboard pattern, white corresponds to maximum, black corresponds to minimum; *C*, random initial conditions.

where $\phi(t)$ is the phase associated with the time series, and t_k are the times of the marker events.

To study synchronization between two oscillators m and n, we use their wrapped phase difference, defined on the interval $[-\pi,\pi]$ [14]:

$$\Phi_{m,n}(t)=[\phi_m(t)-\phi_n(t)]_{mod(2\pi)}. \tag{6}$$

In our study, the following three quantities were used to characterize the dynamics.

1. Average synchronization index

The synchronization index ρ is used to characterize how pronounced the peaks are in the probability distribution p_k of the wrapped phase difference $\Phi_{m,n}$. For example, for a uniform (completely flat) distribution the synchronization index is zero, whereas for a δ function it is equal to 1. The average of several synchronization indices was calculated as follows.

The system was allowed to relax for 15 000 time steps (i.e., 75 time units). During the next 15 000 time steps, the time series of $N=16$ elements were chosen at random and recorded. The average synchronization index was estimated as

$$\rho=\frac{2}{N(N-1)}\sum_{n=1}^{N}\sum_{m<n}\frac{S_{max}-S_{m,n}}{S_{max}}, \tag{7}$$

where S is the Shannon entropy associated with the probability distribution of the phase difference of oscillators m and n:

$$S_{m,n}=-\sum_{k=1}^{N_b}p_k\ln(p_k). \tag{8}$$

In Eq. (8), $N_b=50$ is the number of bins used to determine the probability distribution, and p_k is the probability that the wrapped phase difference $\Phi_{m,n}$ falls into the kth bin. S_{max} is the Shannon entropy corresponding to a uniform distribution,

$$S_{max}=\log_2(50)\approx 5.643\,856. \tag{9}$$

2. Standard deviation of the frequencies

In order to study frequency entrainment, the standard deviation of the frequencies was defined as

$$\sigma_f=\sqrt{\langle f_n^2\rangle-\langle f_n\rangle^2}, \tag{10}$$

where the index n run over the randomly chosen oscillators. The frequency f_n of an oscillator is determined by counting the number of marker events that occur in a unit time. A low value of σ_f indicates frequency entrainment: the oscillators tend to oscillate at a common frequency [19].

3. Standard deviation of the global output

The ''global output'' is the sum of the instantaneous values of $v(i,j,t)$ of all oscillators. Its standard deviation is defined as follows:

$$\sigma_G=\sqrt{\langle G^2(t)\rangle-\langle G(t)\rangle^2},\quad G(t)=\sum_{i,j=1}^{N}v(i,j,t). \tag{11}$$

This quantity defines how much the activity of the individual oscillators is reflected by the entire array. If all elements synchronize, σ_G is maximal and scales with the number of elements N. If the oscillators are uncoupled, σ_G scales with $\sqrt{N}$. In the case of negative coupling, the scaling factor is usually lower than $\sqrt{N}$ (see below).

D. Biological data acquisition

Medial temporal lobe epilepsy tissues were obtained following surgery. Astrocyte cultures were prepared from regions of the brain that correlated to hyperexcitable EEG in the operating room [35]. The cultures were maintained in normal saline. The fluctuations of the calcium ion concentration ($[Ca^{2+}]$) in the tissue were visualized as follows.

(1) The astrocyte culture was placed in a flow-through perfusion chamber and was stained using a calcium-sensitive dye, Fluo-3AM ($2\ \mu M$). The properties of the dye permit visualization of calcium ion concentration (the dye is fluorescent in the presence of free calcium ions). The intensity of the fluorescent light increases with the concentration of free calcium.

(2) The culture was washed out in normal saline, thus the dye remained present only inside the astrocytes.

(3) The probe was placed under a confocal scanning laser microscope (BioRad MRC 500/600). Fluorescent images were collected every 1.8 s using the frame grabber board on the computer (Panasonic 3031TQ). Images were downloaded directly to an optical memory disk recorder. Finally, the results were stored as 480×640 pixel grayscale images, every pixel's values ranging from 0 to 255 (corresponding to black and white, respectively).

(4) Due to the high spatial and temporal noise, the resolution of the images was reduced by computing averages over 11×11 pixel squares centered at every fourth pixel. Thus, the resulting image series were 120×160 pixel grayscale images.

(5) A computational measure, $I(x,y)$ (the intensity of a biological oscillator) was developed to identify the position (x,y) of rapidly oscillating astrocytes. This tool (discussed in Ref. [36]) allows us to select the desired number of most active astrocytes and calculate the synchronization index and standard deviation of the global output as defined in Eqs. (7) and (11), respectively.

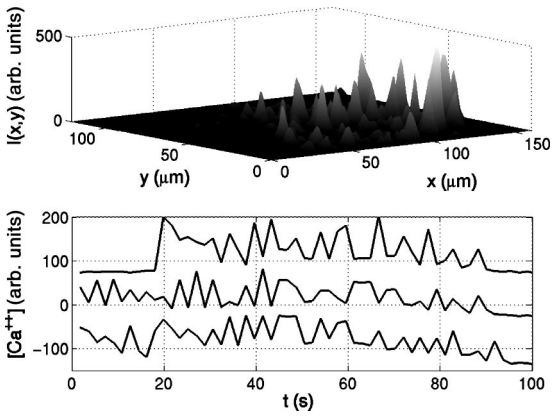

FIG. 4. Experimental data. The map of the intensity of the oscillations can be seen on the top. On the bottom the $[Ca^{2+}]$ time series are shown for the three most active astrocytes. Notice the tendency of peaks to occur either in phase or in antiphase.

The map of the oscillation intensity and the time series of the three most active cells can be seen on Fig. 4. Note that the data are nonstationary and the sampling rate is low (the oscillation period is close to the sampling rate). In order to be able to apply the measures defined above, a running average was subtracted from each time series, and they were all normalized such that finally they had the same standard deviation.

III. RESULTS

A. Application of the statitical measures to the FN array

The numerical results obtained for the three types of initial conditions (*A*, *B*, and *C*) are sumarized in Fig. 5, indicating synchronization for hyperexcitable systems with both phase attractive and phase-repulsive coupling. This is demonstrated by: (1) the increase of the average synchronization index for both positive and negative values of the diffusion coefficient as seen in the first row of graphs (a), (b), and (c), and (2) the decrease of the standard deviation of the frequencies for nonzero values of the diffusion coefficient, shown in the second row of graphs (d), (e), and (f). The first row of graphs indicates phase locking, while the second row indicates frequency entrainment among the oscillators. The third row of graphs (g), (h), and (i) indicates the presence of coupling among the elements of the array. In the following paragraphs, additional analysis is provided for each measure introduced in Sec. II C.

Figure 6 shows the phase difference for three different values of *D*, for several oscillator pairs. The phase differences flatten out due to nonzero coupling.

Figure 7 demonstrates the repulsive character of the coupling, for $D=-0.015$. The probability density of the phase difference is presented, for four oscillators located along a row. Note that the first neighbors tend to be in antiphase, the second neighbors tend to be in phase, the third neighbors tend to be again in antiphase, and so on.

Figure 8 shows the histograms of frequency distribution for three different values of the diffusion coefficient. Note that the increase of (positive or negative) coupling leads to

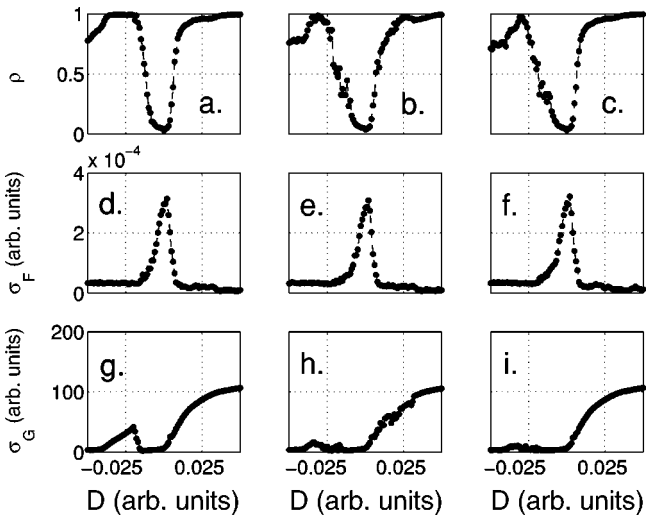

FIG. 5. Results of numerical simulations. (a), (b), and (c), synchronization index as a function of the diffusion coefficient for initial conditions *A*, *B*, and *C*, left-to-right; (d), (e), and (f), standard deviation of frequencies as a function of the diffusion coefficient for inital conditions *A*, *B*, and *C*, respectively; (g), (h), and (i), standard deviation of the global output as a function of the diffusion coefficient for inital conditions *A*, *B*, and *C*, respectively. The results are averages of ten realizations for initial conditions *A* and *B*, and of 40 realizations, for initial conditions *C*. All parameters were chosen as described in Sec. II A. and II B.

clusterization: instead of a uniform distribution of the frequencies, several narrow peaks appear for $D\neq 0$.

The last (third) row of graphs in Fig. 5 indicates that the global output of systems with coupling is different from that of systems with no coupling. It is known that the standard deviation of the sum of statistically independent random processes scales with $\sqrt{N}$, where *N* is the number of processes that are being summed.

This can be verified by looking at the intersection of the last row of curves on Fig. 5 with the $D=0$ vertical line. This intersection is the standard deviation of the global output for

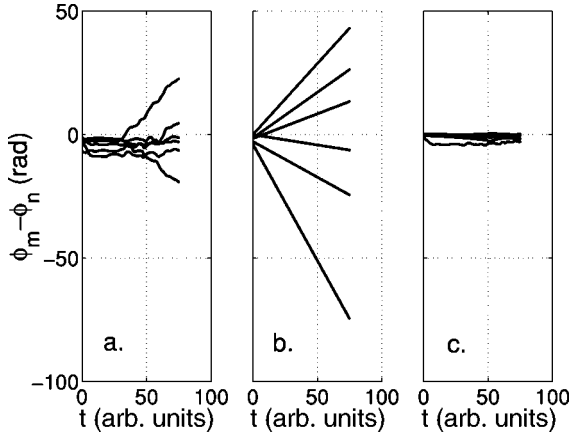

FIG. 6. Phase difference as a function of time for several oscillator pairs. The values of the diffusion coefficient were: (a). $D=-0.006$; (b). $D=0.000$; (c). $D=0.006$. The flat parts of the graphs (slope ≈ 0) indicate a tendency of phase locking.

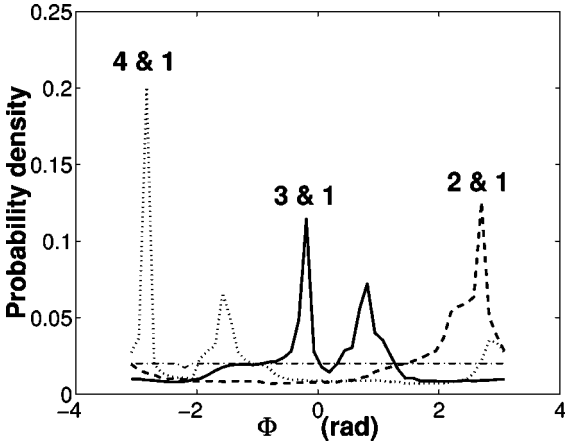

FIG. 7. Probability density of phase difference for four oscillators located in a row ($D=-0.015$). The distributions shown are: nearest neighbors (dashed line); second nearest neighbors (continuous line); third nearest neighbors (dotted line). The dot-dashed line around 0.02 is the phase distribution of the phase difference for a pair of noncoupled cells.

the uncoupled system. If we compare the value of the curves for $D=0$ (≈ 6.3823) with the mean standard deviation of the individual FitzHugh-Nagumo elements (≈ 0.3617), we find $6.3823 \approx 0.3617 \times 18 = 6.5106$, where 18 is the square root of the total number of elements (the borders are excluded because they are responsible for the boundary conditions).

According to our graph, in the presence of (positive or negative) coupling, the standard deviation of the global output differs from its value in the uncoupled case. For positive (or phase-attractive) coupling, the scaling factor is always greater than or equal to $\sqrt{N}$, while for negative (phase-repulsive) coupling, the scaling factor tends to be smaller than $\sqrt{N}$.

This can be seen in more detail in Fig. 9. Also, Figure 10 shows three global outputs for three different diffusion coefficients. Based on the reasoning in the last paragraph, the standard deviation of the global output could become a new testing tool for the presence of coupling in a system of oscillators.

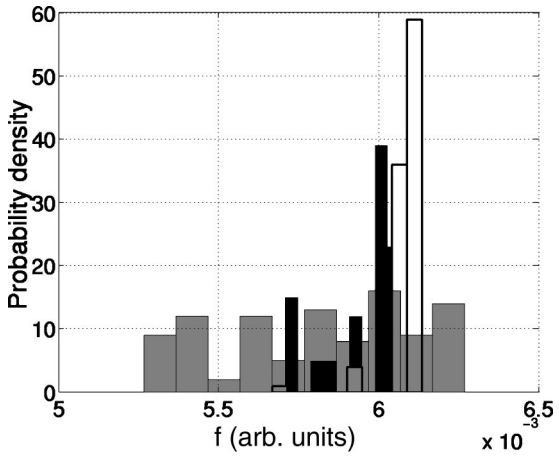

FIG. 8. Probability density histograms of the frequency distribution. The distribution functions are shown for three different values of the diffusion coefficient: $D=-0.010$ (black); $D=0.000$ (gray); and $D=0.008$ (white). The histograms were created by dividing the range between the maximum and minimum values of the frequencies into ten equal-size bins.

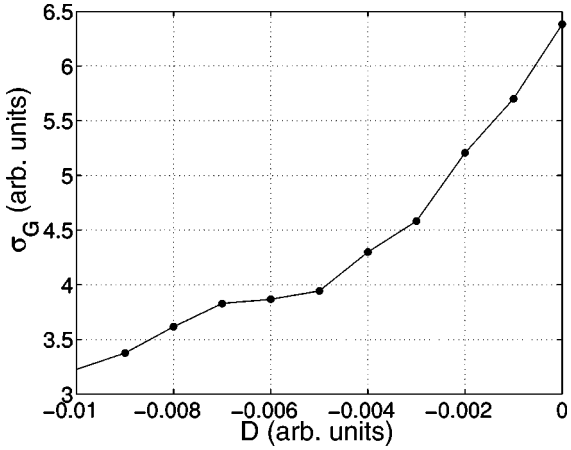

FIG. 9. Standard deviation of the global output for the second type of initial conditions. Notice that for most negative diffusion coefficients (and *only* for negative diffusion coefficients) the standard deviation of the global output is lower than its value for uncoupled systems.

B. Analysis of the experimental data

The average synchronization index ρ [Eq. 7] was calculated from the experimental data and a typical value of 0.15 was found. This would correspond in our simulations to a value of the diffusion coefficient of about $D \approx \pm 0.006$. This fact proves the existence of coupling between the oscillators in the epileptic astrocyte culture. However, the sign of the coupling coefficient D can not be determined from the average synchronization index. Nonetheless, it is possible to use the standard deviation of the global output to determine the sign of the coupling constant D.

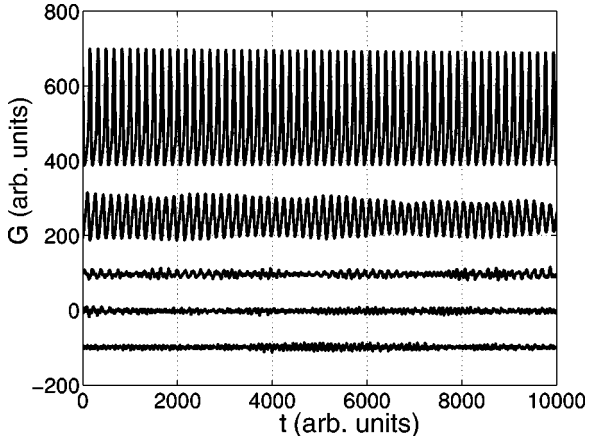

FIG. 10. Global outputs for five different values of the diffusion coefficient (graphs are vertically displaced to make the time series visible). The diffusion coefficients were: $D=-0.010$ (bottom); $D=-0.005$ (second from the bottom); $D=0.000$ (middle); $D=0.005$ (fourth from the bottom); and $D=0.030$ (top).

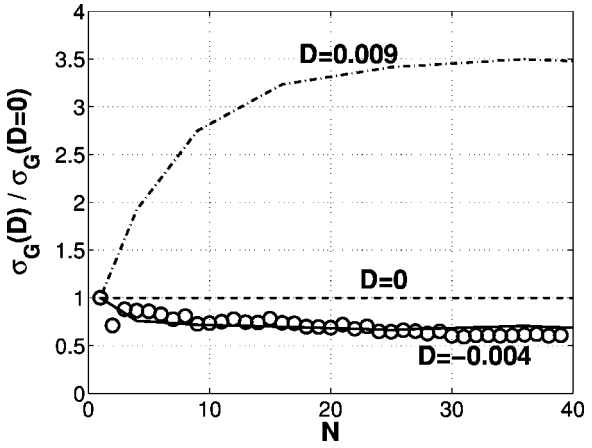

FIG. 11. Ratio of the standard deviation of the global output [σ_G, Eq. 11], to its theoretical value in the case of N random oscillators ($\sqrt{N}\sigma_0$). The dash-dot line represents the result of the simulation with a diffusion coefficient of $D=0.005$; the continuous line represents the results of the simulation for $D=-0.001$ and the circles represent the values calculated from the experimental data. A running average of length 11 time steps was subtracted from the experimental time series. The time series of the calcium fluctuations were also normalized, so that they had the same standard deviation before summation.

If we represent the ratio of the standard deviation of the global output σ_G [Eq. (11)] and its theoretical value in the case of N random oscillators, the results are shown in Fig. 11. The dash-dot line represents the result of the simulation with a diffusion coefficient of $D=0.009$; the continuous line represents the results of the simulation for $D=-0.004$; and the circles represent the values calculated from the experimental data.

Notice that all the values for the experimental data are subunitary. This fact classifies the studied experimental system as having phase-repulsive coulping rather than phase attractive.

The behavior of the simulated system for positive and negative diffusion coefficients reveals interesting patterns. In the regime of positive coupling, the system's elements tend to oscillate together, in phase. This leads to all oscillators reaching their peak almost at the same times. The result is a global output that will be oscillating with the same frequency as the individual oscillators. For strong negative coupling, however, the system's appearance resembles a chessboard, with waves travelling through it (see Fig. 12).

The role of the waves propagating through the system is to periodically change peaks into troughs and vice versa. The more negative the diffusion coefficient, the thinner the wave. In the positive regime, spiral wave patterns are observed and the width of the waves increases with the diffusion coefficient.

For comparison, a temporal sequence of experimental images is shown on Fig. 13. The presence of phase-repulsive coupling is apparent from the fact that when a cell is white (has high $[Ca^{2+}]$), its neighbor becomes black (has low $[Ca^{2+}]$) and vice versa.

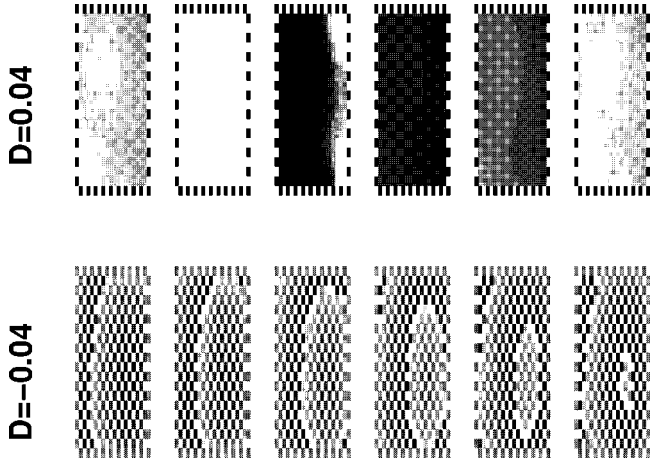

FIG. 12. Temporal sequence of patterns in the systems with nonzero coupling. Time is increasing from left to right, the images are 20 time steps apart. Examples for strong positive coupling (top row) and strong negative coupling (bottom row) are shown. All the parameters were chosen as described in Secs. II A. and II B.

IV. DISCUSSION

The phenomenon of synchronization in systems of many oscillators with phase-repulsive coupling might be ubiquitous in nature. The same is true for its counterpart, the synchronization with phase-attractive coupling. Phase-attractive coupling appears in ''unstressed'' biological systems, while phase-repulsive coupling might be a property of systems under stress, or those whose elements are in competition with each other.

An example could be a group of individuals living in a cave (with no clues of the time outside). The circadian rhythm of each group member is different from all the others, but they will wake up and fall asleep approximately at the same time, to avoid disturbing each other (unstressed system). Notice that in this case there will be times when everybody is awake or everybody is sleeping (and thus the standard deviation of the global output is high, as well as the synchronization index). If there is an external danger, however, and the group has to assign watchers, the situation changes to the opposite. When the watchers get tired, they wake up others to replace them, and thus there will be approximately a constant number of individuals awake and asleep at any time. The synchronization index will be high again, because some people will be awake at the same time, while the others will be asleep at the same time, thus these subgroups will be in an antiphase relation with each other.

Another important example for a phase-repulsive coupled system could be a lipid bilayer (cell membrane) containing voltage-dependent ion channels. In this case, the coupling between the ion channels could be a decrease in voltage across the membrane due to the opening of a channel. This decrease of voltage could increase the probability of ion channel closing in the neighborhood of the open channel.

Further study is needed to give a theoretical explanation of the observed phenomena in the case of phase-repulsive coupling. Systems of other oscillators need to be studied, both experimentally and computationally, because the aspect

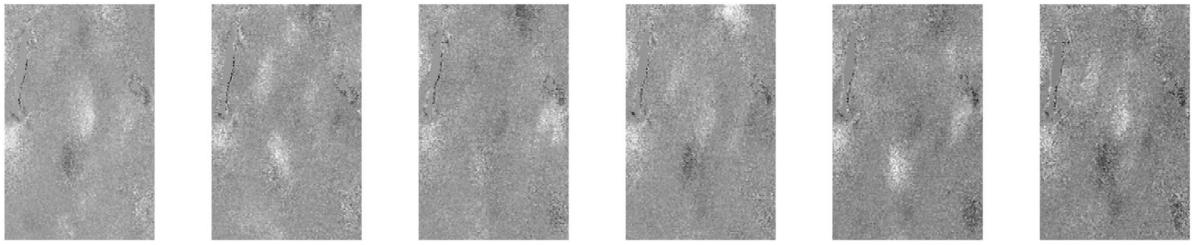

FIG. 13. Temporal sequence of calcium oscillations in an epileptic astrocyte culture. Time is increasing from left to right, time between frames is 1.8 s. Notice the fluctuations of free calcium of the cells in the middle of the images (they oscillate in antiphase).

of the curves on Fig. 5 might depend on the specific type of oscillator chosen. Placing the oscillators on various types of lattices (e.g., triangular instead of square lattice) might result in interesting effects due to frustration.

An important biochemical question is to find the mechanism leading to phase-repulsive coupling in epileptic astrocyte cultures. While the mechanisms leading to calcium wave propagation have been a subject of study and have been reasonably understood, nothing is known about how the intracellular Ca^{2+} dynamics of two cells could influence each other. Our study shows the existence of such an interaction for an epileptic astrocyte culture. Moreover, it has been known that epileptic astrocytes differ in culture from normal astrocytes: the former have increased gap-junctional coupling [35]. This property might play a role in the increased communication between the intracellular events of two astrocytes. However, the actual interaction needs to be worked out, whether it is due to the diffusion of some chemical agent through the extracellular space or to some agent passing through gap junctions.

ACKNOWLEDGMENTS

We thank Zoltán Néda for useful discussions. G.B. is grateful to the Graduate School at the University of Missouri–St. Louis for its support. A.C.-B. acknowledges NIEHS (ESO 8470-04) SBIR phase II grant support. A.N. acknowledges the support of the Fetzer Institute and F.M. acknowledges the support of the Office of Naval Research, Physics Division.

[1] Ch. Huygens (Hugenii), *Horologium Oscillatorium* (Apud F. Muguet, Regis et Archiepiscopi Typographum, Paris, France, 1673), English translation: *The Pendulum Clock* (Iowa State University Press, Ames, 1986).
[2] C. Graves, L. Glass, D. Laporta, R. Meloche, and A. Grassino, Am. J. Physiol. **250**, R902 (1986).
[3] L. Glass and M.C. Mackey, *From Clocks to Chaos: The Rhythms of Life* (Princeton University Press, Princeton, NJ, 1988).
[4] M.G. Rosenblum, A.S. Pikovsky, and J. Kurths, Phys. Rev. Lett. **76**, 1804 (1996).
[5] C. Schäfer, M.G. Rosenblum, H.-H. Abel, and J. Kurths, Phys. Rev. E **60**, 857 (1999).
[6] C. Schäfer, M.G. Rosenblum, H.-H. Abel, and J. Kurths, Phys. Rev. Lett. **76**, 1804 (1996).
[7] C.A. Czeisler, J.F. Duffy, T.L. Shanahan, E.N. Brown, J.F. Mitchell, D.W. Rimmer, J.M. Ronda, E.J. Silva, J.S. Allan, J.S. Emens, D.-J. Dijk, and R.E. Kronauer, Science **284**, 2177 (1999).
[8] A.T. Winfree, *The Geometry of Biological Time* (Springer, Berlin, 1980).
[9] J. Simonet, M. Warden, and E. Brun, Phys. Rev. E **50**, 3383 (1994).
[10] E. Morse, Science **43**, 169 (1916).
[11] G.B. Ermentrout and J. Rinzel, Am. J. Physiol. **246**, R102 (1984).
[12] A. Neiman, X. Pei, D.F. Russell, W. Wojtenek, L. Wilkens, F. Moss, H.A. Braun, M.T. Huber, and K. Voigt, Phys. Rev. Lett. **82**, 660 (1999).
[13] A.B. Neiman, D.F. Russell, X. Pei, W. Wojtenek, J. Twitty, E. Simonotto, B.A. Wettring, E. Wagner, L.A. Wilkens, and F. Moss, Int. J. Bifurcation Chaos Appl. Sci. Eng. **10**, 2499 (2000).
[14] P. Tass, M.G. Rosenblum, J. Weule, J. Kurths, A. Pikovsky, J. Volkmann, A. Schnitzler, and H.-J. Freund, Phys. Rev. Lett. **81**, 3291 (1998).
[15] P.A. Tass, *Phase Resetting in Medicine and Biology. Stochastic Modelling and Data Analysis* (Springer, Berlin, 1999).
[16] A.F. Glova, S.Yu. Kurchatov, V.V. Likhanskii, A.Yu. Lysikov, and A.P. Napartovich, Quantum Electron. **26**, 500 (1996).
[17] V. Petrov, Q. Ouyang, and H.L. Swinney, Nature (London) **388**, 655 (1997).
[18] Z. Néda, E. Ravasz, Y. Brechet, T. Vicsek, and A.-L. Barabási, Nature (London) **403**, 849 (2000).
[19] A. Neiman, L. Schimansky-Geier, A. Cornell-Bell, and F. Moss, Phys. Rev. Lett. **83**, 4896 (1999).
[20] A. Neiman, A. Silchenko, V. Anishchenko, and L. Schimansky-Geier, Phys. Rev. E **58**, 7118 (1998).
[21] A. Neiman, L. Schimansky-Geier, F. Moss, B. Shulgin, and J.J. Collins, Phys. Rev. E **60**, 284 (1999).
[22] H. Hempel, L. Schimansky-Geier, and J. García-Ojalvo, Phys. Rev. Lett. **82**, 3713 (1999).
[23] U. Ernst, K. Pawelzik, and T. Geisel, Phys. Rev. E **57**, 2150 (1998).
[24] C. Sagui and R.C. Desai, Phys. Rev. Lett. **74**, 1119 (1995).
[25] Y. Nakamura, F. Tominaga, and T. Munakata, Phys. Rev. E **49**, 4849 (1994).

[26] R.D. Pinto, P. Varona, A.R. Volkovskii, A. Szücs, H.D.I. Abarbanel, and M.I. Rabinovich, Phys. Rev. E **62**, 2644 (2000).
[27] S. Kunec and A. Bose, Phys. Rev. E **63**, 021908 (2001).
[28] A.H. Cornell-Bell, S.M. Finkbeiner, M.S. Cooper, and S.J. Smith, Science **247**, 470 (1990).
[29] P. Jung, A. Cornell-Bell, K.S. Madden, and F. Moss, J. Neurophysiol. **79**, 1098 (1998).
[30] Z. Wang, P.G. Haydon, and E.S. Yeung, Anal. Chem. **72**, 2001 (2000).
[31] R.D. Fields and B. Stevens, Trends Neurosci. **23**, 625 (2000).
[32] A.H. Cornell-Bell and S.M. Finkbeiner, Cell Calcium **12**, 185 (1991).
[33] R. FitzHugh, Biophys. J. **1**, 445 (1961).
[34] J.S. Nagumo, S. Arimoto, and S. Yoshizawa, Proc. IRE **50**, 2061 (1962).
[35] S.H. Lee, S. Magge, D.D. Spencer, H. Sontheimer, and A.H. Cornell-Bell, Glia **15**, 195 (1995).
[36] G. Balázsi, A.H. Cornell-Bell, A.B. Neiman, and F. Moss (unpublished).